ISSN NO. 2320-5407

Journal homepage: http://www.journalijar.com

INTERNATIONAL JOURNAL OF ADVANCED RESEARCH

RESEARCH ARTICLE

Properties of pure and (Gd,Sm) doped CeO_2 nano-particles

M.H. Khedr[1,2], A.A. Fargali[1,2], W.M.A. El Rouby[2], Ahmed A. Aboud[3] and A.Hamdedein[1]

1 .Chemistry Department, Faculty of Science, Beni-Suef University, Egypt.

2 .Material Science and Nanotechnology Department, Faculty of Postgraduate Studies for Advanced Science, Beni-suef University, Egypt

3 .Physics Department, Faculty of Science, Beni-Suef University, Egypt.

Manuscript Info

Manuscript History:

Received: 18 January 2015
Final Accepted: 12 February 2015
Published Online: March 2015

Key words:

CeO_2; Doping; Gd; Sm; band gap; blue shift; optical properties; hydrothermal.

Corresponding Author

.H. Khedr

Abstract

Pure, Sm and Gd-doped Cerium oxide (ceria) powders have been prepared via hydrothermal technique. All powders were found to be nano-sized particles with particle size lie in the range of 4-16 nm as transmission electron microscope analysis revealed. The particle size was found to be decreased by doping as revealed from TEM images. X-ray diffraction studies show the formation of polycrystalline materials all belongs to cubic ceria phase. No other peaks belongs to separated phase of the dopants were recorded which ensure the good solubility of the dopants on ceria matrix. Small shift in the peak position accompanied with more broadening in Raman analysis is recorded. Optical enegy gaps, transition nature and particle size of the nano-powders all are speculated depending on the optical absorption measurement. The band gas was found fill in the range 6.1 to 5.9 eV in pure and doped powders.

INTRODUCTION

Due to its versatile and tunable properties, metal oxides attract huge interests in academic and industrial fields. CeO_2 is one of the most promising metal oxide [1, 2]. It applications has been extended from gas sensing[3, 4], catalysts[5], fuel cells[3, 4] and fluorescent materials[6]. Therefore, the studies on the preparation and properties of nano-crystalline CeO_2 have attracted extensive interests during the last few years. Nano-crystalline ceria particles have been prepared by hydrothermal [7, 8] , sol-gel [9] and microemulsion [10] techniques.

In the current work nano-particle of pure, 7% Sm and Gd-doped particles have been successfully prepared using hydrothermal techniques. The powders have been characterized and the effect of the doping on the structure has been estimated. Finally Optical band gap value, the nature of transition and the effect of particle size all have been determined.

2. Experimental

Cerium nitrate ($Ce(No_3)_6$), Samarium nitrate hexahydrated, $Sm(NO_3)_2.6H_2O$, gadolinium acetate hydrated ($Gd(AC)_3x.H_2O$) and sodium hydroxide solutions have been used as a starting materials for the powder preparation process. All the reagents were of analytical grade and were used without further purification. In a typical experimental solution of 0.116 M cerium salts is prepared in 100 ml distilled water. Then NaOH (6N) was added drop by drop under stirring for 30 min till complete precipitation of cerium hydroxide. Next, the solution was transferred into Teflon lined

autoclave and the temperature was adjusted to 200°C for 18 h. The precipitate were filtered, washed and dried over night. The solution color changed during the reaction from white to brown and yellow due to the formation of Ce^{4+}[11]. The doped powders were prepared by repeating the previous synthesis scheme and introducing the dopant precursor solutions before the precipitation step. Gadolinium acetate, $Gd(AC)_3x.H_2O$, was used as a source of Gd and Samarium nitrate, $Sm(NO_3)_2.6H_2O$, was used as a source of of Sm. The absorption spectra of all powder samples has been recorded in the spectral wavelength range 190-110nm using double beam spectrophotometer model type T70 provided by PG instruments. All powder samples were suspended in distilled water using quartz cuvette.

X-ray diffraction measurements were conducted on a PANalytical (Empyrean) X-ray diffraction using Cu K_α radiation (wave length 0.154 cm^{-1}) at an accelerating voltage 40 KV and current of 35 mA. FT-Raman spectra were recorded with a Bruker (FTIR-FT Raman) spectrometer with laser beam of 1064 nm power. Transmission Electron microscope images were taken by JEOL-JEM 2100 (Japan) with an acceleration voltage of 200 KV. Double beam spectrophotometer model type T70 provided by PG instruments.

3. Results and discussion

3.1 structure and microstructure study

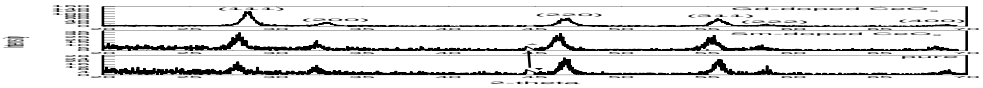

Fig.1:-XRD patterns of CeO_2 nano-particles prepared by hydrothermal method at120°C for 18h: a) pure CeO_2, b) Sm-doped CeO_2 and d) Gd-doped CeO_2.

a)

Fig.1, shows the X-ray diffraction patterns for all prepared nano-powders. As observed the pure cerium oxide powder is power crystalline with (220) as the main peak. This peak is one of the strongest lines in the ICDD card number 04-2965. After the addition of Gd or Sm the preferred orientation was shifted to (111). Also it is observed that the peaks intensities increased by doping.

The average crystallite size of the prepared powder was calculated using Scherrer's formula [18];

$$D = 0.9\lambda/\beta \cos(\theta_\beta) \quad (1)$$

where D is the average crystallite size, λ is the radiation wave length, β is the full-width at half-maximum, and θ_β is the Bragg's angle. The size was found to be decreased as a result of doping.

3.2 Transmission electron microscope examination.

Fig.2 (a, b and c) shows TEM images of pure, Sm and Gd-doped CeO_2, respectively. It is clearly observed that all samples had polygonal shapes although nano-sized Gd_2O_3 doped CeO_2 had more dispersal structure and nearly most particles have cubic structure with average particle size about (6.6-14.7) nm while nano-sized Sm_2O_3 doped CeO_2 has average particle size of (4.6-12.44) nm while pure cerium oxide has larger averaparticle size about (10.7-16.8) nm with dense and agglomerated structure.

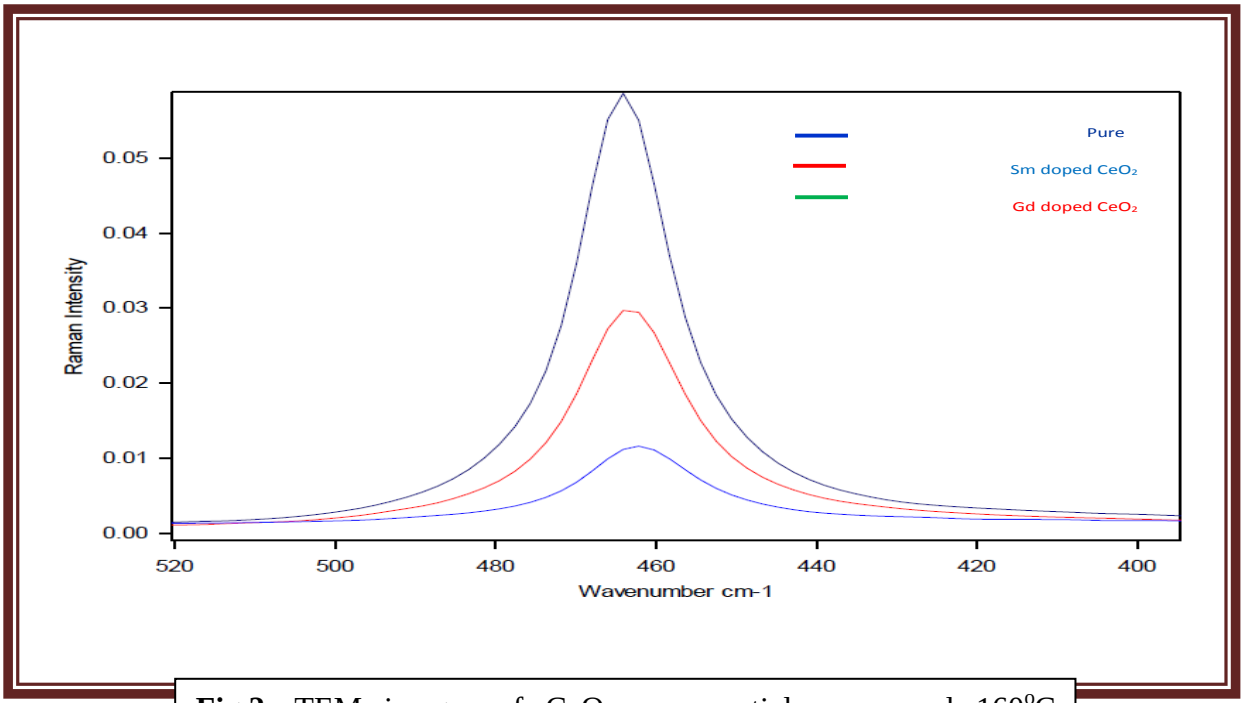

Fig.2. TEM images of CeO_2 nano-particles prepared 160^oC for 18h using cerium nitrate as a precursor materials: a) pure CeO_2, b) Sm-doped CeO_2 and c) Gd-doped CeO_2.

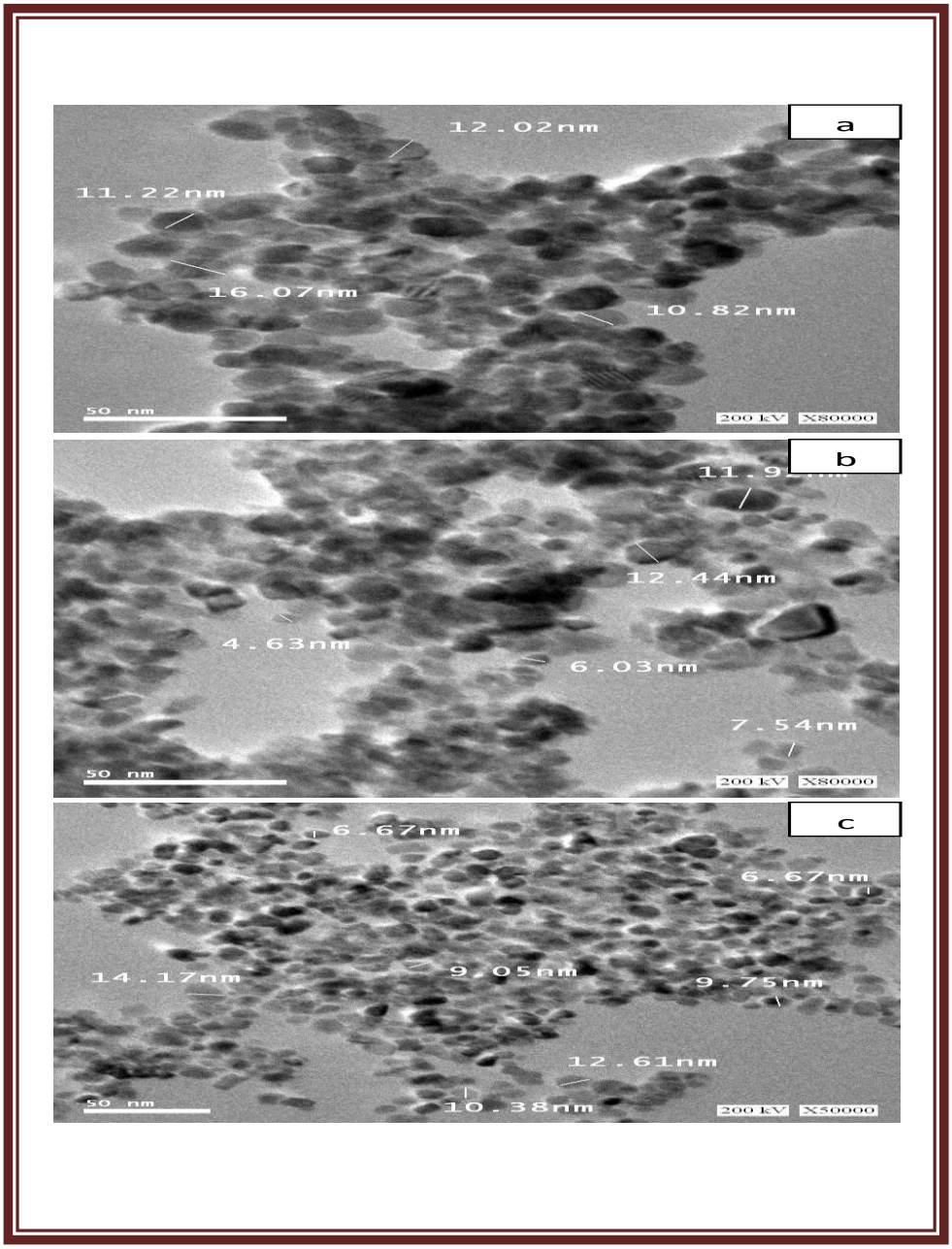

3.3 Raman spectroscopy.

Raman spectra of hydrothermally synthesized CeO_2, Gd doped CeO_2 and Sm doped CeO_2 powders are illustrated in Fig.3, which confirm the formation of the polygonal fluorite phase. The intensive band at 450–470cm^{-1} corresponding to the allowed Raman mode (F_{2g}) of fluorite metal dioxides belonged to the O^5_h (Fm3m) space group [12-14]. For pure CeO_2 powders, the Raman spectrum was symmetric around 464 cm^{-1} and the F_{2g} mode corresponded

to the symmetric vibration of oxygen ions around Ce^{4+} ions [14]. In the samarium and gadolinium doped CeO_2, the F_{2g} band became asymmetrical and slightly shifted to low frequencies, due to the cell expansions resulting from the substitution of Sm^{3+} and Gd^{3+}ions in the CeO_2 lattices and the subsequent oxygen loss around cations.

3.4 Optical properties and band gap values.

In this section of the study the optical properties of the pure, Sm and Gd-doped CeO_2 has been investigated. Optical band gap value, the nature of the transition and the effect of particle size all have been determined. The absorbance data has been utilized to determine the absorption coefficient according to the following equation [15-17] ;

$$\alpha = \frac{2.303\ x\ 10^3\ A\ \beta}{lc}$$

Where A is the absorbance of the sample, β is the density of Ceo_2 (7.172g/cm^3), L is the path of the quartz cell (1.0cm), and c is he concentration of the powder in the suspension.

Based on direct allowed transition type the optical band gap of all powder samples were investigated using Tauc's equation [18]'

$$\alpha = A\frac{(h\nu - E_g)^{1/2}}{h\nu}$$

The band gap value was determined by extrapolating the intercept the hv axe. The intersection point is considered as the band gap value Fig.4.

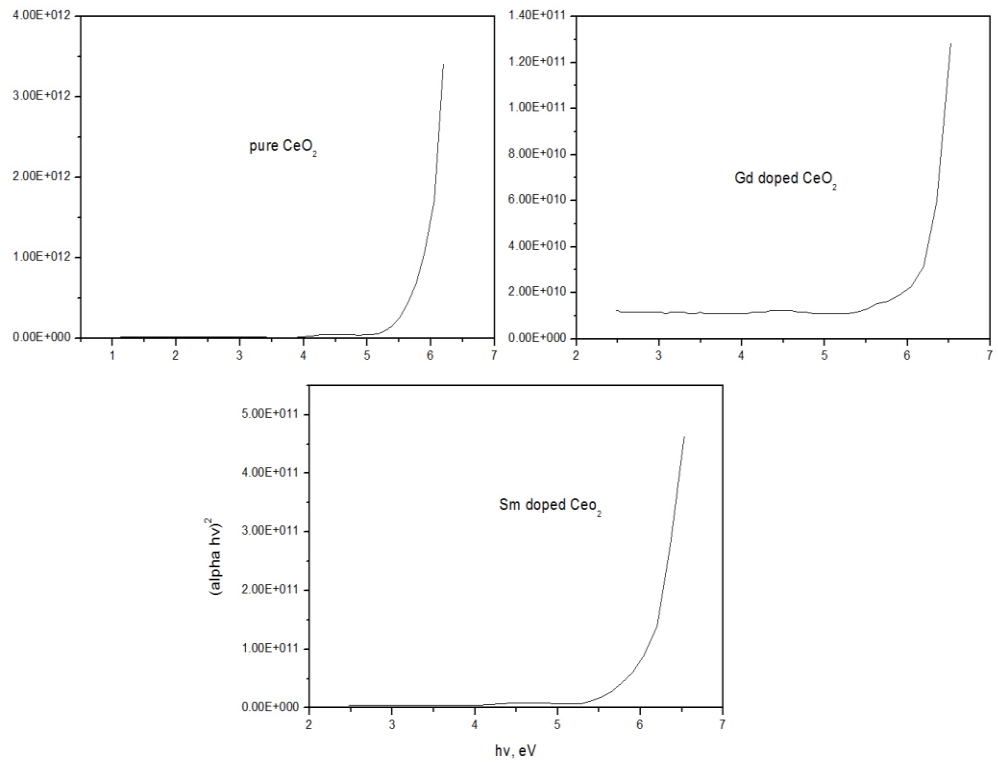

Table 1: Band gap energies, blue-shifts and their relation with the crystal size for pure CeO_2 Sm doped CeO_2 and Gd doped CeO_2 nanoparticles.

Sample	Band gap (eV)	Crystal size calculated (nm)	Average crystal size measured by TEM (nm)
Pure CeO_2	5.97	3.17	(10.8-16.07)
Sm doped CeO_2	6.09	3.1	(4.63-12.44)
Gd doped CeO_2	6.1	3.05	(6.67-14.17)

Table 1 shows the corded values of the band gap with the particle size obtained by different means. As listed in the table the recorded Eg value for the CeO_2 is about 6.1eV which higher than the recorded value of bulk CeO_2 [19, 20] .Such result could be attributed to the small particle size which approach Boher radius (3nm [38, 39]). The particle size of the prepared powder where determined using the band gap value according to [21].

$E_{g.eff} = E_{g,b} + \pi h^2/2R^2 (1/m^*_e + 1/m^*_h) - 1.8e^2/ER$

Where $E_{g,b}$ is the bulk band gap energy (3.19) eV, R is the particle radius, m^*_e and m^*_h are the effective mass of the electron and the hole, respectively, with $m^*_e = m^*_h = 0.04\ m_0$($m_0$ the mass of a free electron), h is planck's constant, and E is the bulk optical dielectric constant. The data obtained from the above equation proves that obtained from TEM at which the doped CeO_2 have average particle size smaller than of pure nano- sized CeO_2. As the crystal size decrease the band gap energy will increase. When the crystallinity decrease from 82% to 18% the band gap energy increased from 2.83 eV to 3.03 eV. Table 1 contains the band gap values of the entire samples. Pure CeO_2, Gd and Sm- doped CeO_2 exhibit a band gap values of 5.97 eV, 6.1 eV and 6.09 eV, respectively that are higher than that of the bulk value 3.15 eV. i.e blue shifted. As mentioned above the blue shift occurs due to quantum confinement and the concentration of Ce^{+3} in the grain boundary decrease by doping, so the band gap energy increase. The absorption band in UV region occur due to the charge transfer between O 2P and 4f-Ce. At small doping ratio the dopant element (Sm and Gd) creates ground and excited f-energy states in the mild band gap of CeO_2, these energy states of (Sm and Gd) take up nany of the excited electrons coming from O 2P level . This ultimately leads to reduction in the band gap. However, at higher doping ratio the band gap is again increased. Increase in the band gap at this concentration can be related to Burstein-Moss (BM) shift[22].

$E_g^{BM} = h2/2m^*_{vc} (3\pi^2 n_e)^{2/3}$

Where m^*_{vc} effective mass of the electrons, ne is is the electron concentration, h is the plank constant. According to BM effect, above Mott critical density, the increased number of free electron concentration need to partial filling of 4f level, which in turn blocks the lowest state and lead to band gap widening [23]. The crystatallite size decrease to 3.05 nm at 7% doping. The carriers will be more confined in the small sized particles, increasing the energy gap of the nanoparticles. Therefore, both small particle size and BM effect result in increase in the band gap.

4. Conclusion

Pure Sm and Gd-doped CeO2 nano-powder have been successfully prepared using hydrothermal technique. The formation of single phase is confirmed by XRD and Raman spectroscopy data. The particle size was measured using Sherrer's equation and TEM measurement. Both techniques revealed that the particle size decreased as a result of doping. Finally Pure, Gd and Sm-doped CeO_2 exhibit band gap values of 5.97 eV, 6.1 eV and 6.09 eV, respectively which are higher than that of the bulk value 3.15 eV. i.e blue shifted.

5. References

1. Hirai, T., et al., *Characterization of metal/ferroelectric/insulator/semiconductor structure with CeO2 buffer layer*. Japanese journal of applied physics, 1995. **34**(8R): p. 4163.

2. Kim, Y.T. and D.S. Shin, *Memory window of Pt/SrBi 2 Ta 2 O 9/CeO 2/SiO 2/Si structure for metal ferroelectric insulator semiconductor field effect transistor.* Applied Physics Letters, 1997. **71**(24): p. 3507-3509.
3. Izu, N., W. Shin, and N. Murayama, *Fast response of resistive-type oxygen gas sensors based on nano-sized ceria powder.* Sensor Actuat B-Chem, 2003. **93**(1–3): p. 449-453.
4. Cui, Q., et al., *Direct fabrication of cerium oxide hollow nanofibers by electrospinning.* J Rare Earth, 2008. **26**(5): p. 664-669.
5. Ismagilov, Z.R., E.V. Matus, and L.T. Tsikoza, *Direct conversion of methane on Mo/ZSM-5 catalysts to produce benzene and hydrogen: achievements and perspectives.* Energ Environ Sci 2008. **1**(5): p. 526-541.
6. García-Melchor, M. and N. López, *Homolytic Products from Heterolytic Paths in H2 Dissociation on Metal Oxides: The Example of CeO2.* The Journal of Phys Chem C, 2014. **118**(20): p. 10921-10926.
7. Wu, N.C., et al., *Effect of pH of medium on hydrothermal synthesis of nanocrystalline cerium (IV) oxide powders.* Journal of the American Ceramic Society, 2002. **85**(10): p. 2462-2468.
8. Kaneko, K., et al., *Structural and morphological characterization of cerium oxide nanocrystals prepared by hydrothermal synthesis.* Nano letters, 2007. **7**(2): p. 421-425.
9. Yu, T., et al., *Large‐Scale Nonhydrolytic Sol–Gel Synthesis of Uniform‐Sized Ceria Nanocrystals with Spherical, Wire, and Tadpole Shapes.* Angewandte Chemie, 2005. **117**(45): p. 7577-7580.
10. Sanchez-Dominguez, M., M. Boutonnet, and C. Solans, *A novel approach to metal and metal oxide nanoparticle synthesis: the oil-in-water microemulsion reaction method.* Journal of nanoparticle research, 2009. **11**(7): p. 1823-1829.
11. Suresh, R., V. Ponnuswamy, and R. Mariappan, *Effect of annealing temperature on the microstructural, optical and electrical properties of CeO< sub> 2</sub> nanoparticles by chemical precipitation method.* Applied Surface Science, 2013. **273**: p. 457-464.
12. Li, G., R.L. Smith, and H. Inomata, *Synthesis of Nanoscale Ce1-xFexO2 Solid Solutions via a Low-Temperature Approach.* J Am Chem Soc, 2001. **123**(44): p. 11091-11092.
13. Singh, P. and M.S. Hegde, *Ce0.67Cr0.33O2.11: A New Low-Temperature O2 Evolution Material and H2 Generation Catalyst by Thermochemical Splitting of Water†.* Chem Mater, 2009. **22**(3): p. 762-768.
14. Kosacki, I., et al., *Raman scattering and lattice defects in nanocrystalline CeO2 thin films.* Solid State Ionics, 2002. **149**(1–2): p. 99-105.
15. Ko, H.-H., et al., *Isothermal crystallization kinetics and effect of crystallinity on the optical properties of nanosized CeO< sub> 2</sub> powder.* Ceramics International, 2014. **40**(5): p. 6663-6671.
16. Maensiri, S., et al., *Egg White Synthesis and Photoluminescence of Platelike Clusters of CeO2 Nanoparticles.* Crystal Growth & Design, 2007. **7**(5): p. 950-955.
17. Taguchi, M., et al., *Supercritical hydrothermal synthesis of hydrophilic polymer-modified water-dispersible CeO2 nanoparticles.* CrystEngComm, 2011. **13**(8): p. 2841-2848.
18. Chrysicopoulou, P., et al., *Optical properties of very thin (< 100 nm) sol–gel TiO< sub> 2</sub> films.* Thin Solid Films, 1998. **323**(1): p. 188-193.
19. Tsunekawa, S., T. Fukuda, and A. Kasuya, *Blue shift in ultraviolet absorption spectra of monodisperse CeO2− x nanoparticles.* Journal of applied physics, 2000. **87**(3): p. 1318-1321.
20. Patsalas, P., S. Logothetidis, and C. Metaxa, *Optical performance of nanocrystalline transparent ceria films.* Applied Physics Letters, 2002. **81**(3): p. 466-468.
21. Goharshadi, E.K., S. Samiee, and P. Nancarrow, *Fabrication of cerium oxide nanoparticles: characterization and optical properties.* Journal of colloid and interface science, 2011. **356**(2): p. 473-480.
22. Muñoz, M., et al., *Burstein-Moss shift of n-doped In 0.53 Ga 0.47 A s/I n P.* Physical Review B, 2001. **63**(23): p. 233302.
23. Vdovenko, V., G. Romanov, and V. Shcherbakov, *BAND SHIFT IN U (IV) ABSORPTION SPECTRA DURING FORMATION OF FLUORINE COMPLEXES.* Resonance, 1993: p. 7.